Author Manuscript

Author Manuscript

Author Manuscript

Author Manuscript

HHS Public Access

Author manuscript

Nat Med. Author manuscript; available in PMC 2016 February 01.

Published in final edited form as:

Nat Med. 2015 August ; 21(8): 932–937. doi:10.1038/nm.3898.

β2-microglobulin is a systemic pro-aging factor that impairs cognitive function and neurogenesis

Lucas K. Smith[1,2,3,*], **Yingbo He**[4,*], **Jeong-Soo Park**[4,5,*], **Gregor Bieri**[1,2,4,6,*], **Cedric E. Snethlage**[1,2,*], **Karin Lin**[1,2,7], **Geraldine Gontier**[1,2], **Rafael Wabl**[4], **Kristopher Plambeck**[1,2], **Joe Udeochu**[1,2,3], **Elizabeth G. Wheatley**[1,2,8], **Jill Bouchard**[1,2], **Alexander Eggel**[9], **Ramya Narasimha**[4], **Jacqueline L. Grant**[4,6], **Jian Luo**[4], **Tony Wyss-Coray**[4,6,10], and **Saul A. Villeda**[1,2,3,7,8,11,#]

[1]Department of Anatomy, University of California San Francisco, San Francisco, California, USA [2]The Eli and Edythe Broad Center for Regeneration Medicine and Stem Cell Research, San Francisco, California, USA [3]Biomedical Sciences Graduate Program, University of California San Francisco, San Francisco, California, USA [4]Department of Neurology and Neurological Sciences, Stanford University School of Medicine, Stanford, California, USA [5]Department of Biochemistry, Dankook University College of Medicine, Cheonan, Korea [6]Neuroscience IDP Graduate Program, Stanford University School of Medicine, Stanford, California, USA [7]Neuroscience Graduate Program, University of California San Francisco, San Francisco, California, USA [8]Developmental and Stem Cell Biology Graduate Program, University of California San Francisco, San Francisco, California, USA [9]Department of Rheumatology, Immunology and Allergology, University Hospital Bern, Bern Switzerland [10]Center for Tissue Regeneration, Repair and Restoration, VA Palo Alto Health Care System, Palo Alto, California, USA [11]California Institute for Qualitative Biosciences (QB3), San Francisco, California, USA

Aging drives cognitive and regenerative impairments in the adult brain, increasing susceptibility to neurodegenerative disorders in healthy individuals[1–4]. Experiments using heterochronic parabiosis, in which circulatory systems of young and old animals are joined, indicate that circulating pro-aging factors in old blood drive aging phenotypes in the brain[5,6]. Here we identify β2-microglobulin (B2M), a component of major histocompatibility complex class 1 (MHC I) molecules, as a circulating factor that negatively regulates cognitive and regenerative function in the adult hippocampus in an age-dependent manner. B2M is elevated in the blood of aging humans and mice, and is increased

Users may view, print, copy, and download text and data-mine the content in such documents, for the purposes of academic research, subject always to the full Conditions of use:http://www.nature.com/authors/editorial_policies/license.html#terms

[#]Corresponding Author saul.villeda@ucsf.edu.
[*]The authors contributed equally

Author contributions

L.K.S, J-S.P, G.B, C.E.S., S.A.V performed pharmacological studies. L.K.S, Y.H, J-S.P, C.S., S.A.V analyzed knockout studies. L.K.S, G.B, C.S., K.L, S.A.V performed behavioral studies. L.K.S., C.S., K.L., G.G., K.P. J.U., J.L. performed parabiosis studies. L.K.S performed biochemical studies. Y.H., J-S. P performed *in vitro* studies. A.E, S.A.V analyzed human data. R.W, E.G.W., J.B, R.N, J.G assisted in histological analysis. G.B generated schematics. S.A.V and T.W.C developed the concept. S.A.V wrote manuscript and supervised study. All authors had the opportunity to discuss results and comment on the manuscript.

Competing financial interests

The authors declare that they have no competing financial interests.

Author Manuscript Author Manuscript Author Manuscript Author Manuscript

within the hippocampus of aged mice and young heterochronic parabionts. Exogenous B2M injected systemically, or locally in the hippocampus, impairs hippocampal-dependent cognitive function and neurogenesis in young mice. Negative effects of B2M, and heterochronic parabiosis, are in part mitigated in the hippocampus of young transporter associated with antigen processing 1 (Tap1)-deficient mice with reduced surface expression of MHC I. Absence of endogenous B2M expression abrogates age-related cognitive decline and enhances neurogenesis in aged mice. Our data indicate that systemic B2M accumulating in aging blood promotes age-related cognitive dysfunction and impaired neurogenesis, in part via MHC I, suggesting B2M may be targeted in old age.

Aging remains the most dominant risk factor for dementia-related neurodegenerative diseases, such as Alzheimer's disease[1–3]. As such, it is imperative to gain mechanistic insight into what drives aging phenotypes in the brain in order to counteract vulnerability to cognitive dysfunction. We, and others, have shown that heterochronic parabiosis or young plasma administration can partially reverse age-related loss of cognitive and regenerative faculties in the aged brain[5–7]. Heterochronic parabiosis studies have revealed an age-dependent bi-directionality in the influence of the systemic environment indicating pro-youthful factors in young blood elicit rejuvenation while pro-aging factors in old blood drive aging[5,6,8–10]. It has been proposed that mitigating the effect of pro-aging factors may also provide an effective approach to rejuvenate aging phenotypes[7,11,12]. To that end, we previously identified a subset of blood-borne immune-related factors, including B2M, as potential pro-aging factors[6]. However, the functional involvement of B2M in mediating age-related impairments in the adult brain, or the potential benefit of abrogating B2M expression during aging, has not been investigated.

B2M comprises the light chain of MHC I molecules that form an active part of the adaptive immune system[13]. In the brain, B2M and MHC I can act independent of their canonical immune function to regulate normal brain development, synaptic plasticity and behavior[14–20]. Increased systemic levels of soluble B2M have been implicated in cognitive impairments associated with chronic hemodialysis[21,22]. Moreover, increased soluble B2M has also been detected in the cerebral spinal fluid (CSF) of patients with HIV-dementia[23,24] and Alzheimer's disease[25]. Considering the association between systemic B2M levels and cognitive decline, and having identified B2M as a potential pro-aging factor associated with decreased neurogenesis[6], we hypothesized that B2M contributes to age-related cognitive and regenerative impairments in the adult brain.

We characterized changes in the concentration of B2m in mouse plasma during normal aging (Fig. 1a), and in the experimental aging model of heterochronic parabiosis (Fig. 1b). We observed an increase in the concentration of B2m in plasma derived from aged (18 and 24 months) compared to young (3 months) animals (Fig. 1a), and plasma derived from young (3 months) heterochronic parabionts after exposure to aged (18 months) blood compared to age-matched young isochronic parabionts (Fig. 1b). Additionally, we detected an age-related increase in the concentration of B2M measured in archived plasma and CSF samples from healthy individuals between 20 and 90 years of age (Fig. 1c,d; Supplementary Table 1).

Author Manuscript Author Manuscript Author Manuscript Author Manuscript

Next we tested whether increasing B2M systemically could elicit cognitive impairments reminiscent of age-related dysfunction. As a control, we assessed hippocampal-dependent learning and memory using radial arm water maze (RAWM) and contextual fear conditioning paradigms in a cohort of young (3 months) and aged (18 months) untreated animals and observed age-related cognitive impairments (Supplementary Figure 1a–e). Subsequently, we tested cognitive function in young (3 months) adult mice systemically administered soluble B2M protein (100 ug/kg) or vehicle via intraorbital injections five times over 12 days (Fig. 1e). Animals showed no signs of illness or weight loss regardless of treatment (Supplementary Fig. 2a). During RAWM training all mice showed similar swim speeds (Supplementary Fig. 2b) and learning capacity for the task (Fig. 1e). However, during testing animals receiving B2M exhibited impaired learning and memory, committing more errors in locating the target platform than animals receiving vehicle control (Fig. 1e). During fear conditioning training all mice exhibited no differences in baseline freezing time (Supplementary Fig. 2c). However, mice receiving B2M demonstrated decreased freezing time during contextual (Fig. 1e), but not cued (Supplementary Fig. 2d), memory testing compared to vehicle treated control animals.

Impairments in hippocampal-dependent learning and memory have been previously linked with decreased adult neurogenesis[26–28]. While a causal link between age-related cognitive decline and decreased adult neurogenesis remains obfuscated[29–32], recent studies using heterochronic parabiosis indicate that cognitive changes elicited by blood from aged rodents are associated with corresponding changes in adult neurogenesis[5,6]. Consequently, we investigated whether increased systemic exposure to B2M decreased adult hippocampal neurogenesis. Using immunohistochemical analysis we detected a significant decrease in the number of Doublecortin (Dcx)-positive newly born neurons (Fig. 1f,g), Nestin-positive progenitors (Supplementary Fig. 3a), Mcm2-postive progenitors (Supplementary Fig. 3b), and proliferating cells having incorporated Bromodeoxyuridine (BrdU; Supplementary Fig. 3c) in the dentate gyrus (DG) of mice systemically administrated exogenous B2M compared to mice injected with vehicle control. As a negative control, we previously demonstrated that systemic administration of monocyte colony stimulating factor (M-CSF), a protein that is not altered in plasma with age, does not elicit changes in adult neurogenesis[6].

To determine whether systemic age-related changes in B2m levels were also accompanied by local changes within the brain, we measured B2m levels within the hippocampus of young (3 months) and aged (18 months) animals by Western blot analysis and detected an age-related increase in B2m protein expression (Fig. 2a). Similarly, systemic changes in the levels of B2m, elicited by exposure to an aged (18 months) systemic environment, were also associated with a corresponding increase in B2m protein expression in the hippocampal lysates of young (3 months) heterochronic parabionts compared to age-matched young isochronic parabionts (Fig. 2b).

To test the effect of local exposure to exogenous B2M on learning and memory we administered a single dose of B2M or a vehicle to young (3 months) adult mice by bilateral stereotaxic injections followed six days later by cognitive testing using RAWM and contextual fear conditioning (Fig. 2c). All mice showed similar swim speeds (Supplementary Fig. 4a) and learning capacity (Fig. 2c) during RAWM training. During

Author Manuscript Author Manuscript Author Manuscript Author Manuscript

testing animals receiving B2M committed more errors in locating the target platform than animals receiving vehicle control (Fig. 2c). During fear conditioning training no mice exhibited differences in baseline freezing time (Supplementary Fig. 4b). However, mice receiving B2M demonstrated decreased freezing time during contextual (Fig. 2c), but not cued (Supplementary Fig. 4c), memory testing. To investigate how persistent the effects of B2M are on cognitive function we administered a single dose of B2M or a vehicle to an independent cohort of young (3 months) adult mice by bilateral stereotaxic injections followed 30 days later by cognitive testing using RAWM and contextual fear conditioning (Fig. 2d). Impairments in hippocampal-dependent learning and memory after local B2M administration were no longer apparent following this extended recovery period (Fig. 2d; Supplementary Fig. 4d–f), indicating the negative effects of B2M on cognitive function are not sustained and potentially reversible.

Given B2M is an active component of the MHC I complex through non-covalent interactions on the cell surface, we investigated whether surface MHC I expression mediates the negative effects of exogenous B2M on cognitive function. Tap1 protein is required for transport of MHC I molecules, and absence of Tap1 results in very few classical MHC I molecules reaching the cell surface[16,17,33]. Therefore, we administered B2M or vehicle control to young (3 months) adult *Tap1* knockout mice (*Tap1*$^{-/-}$) by bilateral stereotaxic injections followed six days later by cognitive testing using RAWM and contextual fear conditioning (Fig. 2e). Local administration of B2M did not alter hippocampal-dependent learning and memory in *Tap1*$^{-/-}$ as compared to vehicle-injected *Tap1*$^{-/-}$ mice (Fig. 2e; Supplementary Fig. 5a–c). Consistent with previous reports[34], we observed no differences in learning and memory between young adult *Tap1*$^{-/-}$ and wild type (WT) littermates (Supplementary Fig. 6a–e).

To examine the effect of local exposure to exogenous B2M in the brain, we stereotaxically injected B2M into the right DG and vehicle control into the left contralateral DG of young (3 months) adult mice (Fig. 2f). Local exposure of the DG to B2M resulted in a decrease in the number of Dcx-positive newly born neurons (Fig. 2g,h), Nestin-positive progenitors (Supplementary Fig. 7a), and Tbr2-positive progenitors (Supplementary Fig. 7b) compared with the contralateral DG treated with vehicle control. Additionally, we investigated the effects of B2M *in vitro*. Exposure of primary mouse hippocampal neural progenitor cells (NPCs) to soluble B2M decreased self-renewal, proliferation, and neuronal differentiation, in the absence of cytotoxicity (Supplementary Fig. 8a–g).

To test whether decreased surface MHC I expression could also mitigate the inhibitory effect of exogenous B2M at a cellular level, we stereotaxically injected young (3 months) adult *Tap1*$^{-/-}$ mice with B2M into the right DG and vehicle control into the left contralateral DG (Fig. 2f). No difference in the number of Dcx-positive (Fig. 2g,i), Nestin-positive (Supplementary Fig. 9a), or Tbr2-positive (Supplementary Fig. 9b) cells was detected between the B2M treated DG compared to the control treated DG of *Tap1*$^{-/-}$ mice. Consistent with previous reports[34], we observed no differences in baseline levels of neurogenesis between young adult *Tap1*$^{-/-}$ and wild type (WT) littermates (Supplementary Fig. 10a–c). Additionally, *in vitro*, we observed no changes in self-renewal after exposure to

Author Manuscript Author Manuscript Author Manuscript Author Manuscript

B2M in primary mouse hippocampal NPCs derived from *Tap1*$^{-/-}$ mice (Supplementary Fig. 8h).

Next, we sought to investigate whether decreasing surface MHC I expression could also mitigate in part the negative effects of aged blood on adult neurogenesis elicited by heterochronic parabiosis (Fig. 3a). Consistent with previous reports[5,6], we observed a decrease in the number of Dcx-positive immature neurons (Fig. 3b,c), Tbr2-positive progenitors (Supplementary Fig. 11a,b), and BrdU-positive proliferating cells (Fig. 3d) in young (3 months) WT heterochronic parabionts (exposed to an aged circulation) compared to age-matched young WT isochronic parabionts. In contrast, there was no significant difference in the levels of neurogenesis in young (3 months) *Tap1*$^{-/-}$ heterochronic parabionts (Fig. 3b–d; Supplementary Fig. 11b). As a control, no changes in neurogenesis were detected between young WT and young *Tap1*$^{-/-}$ isochronic parabionts (Supplementary Fig. 12b–d).

Lastly, we investigated the potential benefit of reducing endogenous B2m expression on age-related cognitive decline. We assessed hippocampal-dependent learning and memory in young (3 months) and aged (17 months) *B2m* knockout mice (*B2m*$^{-/-}$) and WT controls using RAWM and contextual fear conditioning. In young animals no difference in spatial learning and memory were observed between *B2m*$^{-/-}$ and WT controls during RAWM training or testing (Fig. 4a). Aged *B2m*$^{-/-}$ mice showed enhanced spatial learning capacity during RAWM training, as well as enhanced learning and memory for platform location during testing compared to WT controls (Fig. 4c). Animals in each age group showed no differences in swim speed regardless of genotype (Supplementary Fig. 13a,d). During fear conditioning training, all mice exhibited similar baseline freezing independent of genotype (Supplementary Fig. 13b,e). Additionally, no difference in freezing was observed in young *B2m*$^{-/-}$ and WT mice during either contextual (Fig. 4b) or cued fear conditioning (Supplementary Fig. 13c) paradigms. However, aged *B2m*$^{-/-}$ mice demonstrated significantly increased freezing in contextual (Fig. 4d), but not cued (Supplementary Fig. 13f) memory testing compared to WT controls.

Subsequently, we investigated whether absence of endogenous B2m could also counteract age-related declines in adult neurogenesis. We examined changes in neurogenesis in young (3 months) and aged (17 months) adult *B2m*$^{-/-}$ and WT littermates by immunohistochemical analysis. In young adult animals the absence of endogenous B2m expression had no effect on the number of Dcx-positive newly born neurons (Fig. 4e,f) or BrdU-positive proliferating cells (Supplementary Fig. 14a). However, in aged *B2m*$^{-/-}$ mice there was an increase in the number of Dcx-positive (Fig. 4e,g) and BrdU-positive (Supplementary Fig. 14b) cells compared to WT littermates. Subsequently, we assessed neuronal differentiation and survival in *B2m*$^{-/-}$ mice using a long-term BrdU incorporation paradigm, in which mature differentiated neurons express both BrdU and the neuronal marker NeuN (Fig. 4h). Young adult *B2m*$^{-/-}$ mice showed no differences in neuronal differentiation (Fig. 4i), while aged adult *B2m*$^{-/-}$ mice showed a significant increase compared to age-matched WT littermates (Fig. 4j). No differences were detectable in astrocyte differentiation at any age as quantified by the percentage of cells expressing BrdU and GFAP markers (Supplementary Fig. 14c–e).

Author Manuscript Author Manuscript Author Manuscript Author Manuscript

B2M in concert with MHC I molecules continue to be demonstrated to have a unique involvement in the CNS[14,16–20], with previous studies implicating a protective effect of abrogating MHC I expression in brain injury models such as stroke[35]. Our study elucidates a previously unrecognized role for B2M in the progression of age-related impairments in both cognitive and regenerative processes. Moreover, our study implicates surface MHC I expression in mediating, in part, the negative effects of B2M and heterochronic parabiosis. Notably, human genome-wide association studies (GWAS) have linked the MHC locus on chromosome 6p21 with degenerative diseases of aging, further suggesting an active role for these molecules in age-dependent impairments[36]. It should be noted that at present our data does not distinguish between the effects of MHC I expression at the systemic versus local levels. Therefore it is important to investigate how the more than 50 MHC I molecules[17] may alter cognitive and regenerative function in the aging brain through both canonical immune and non-canonical neurogenic regulation of processes including neurogenesis and synaptic plasticity. Notwithstanding, our data provide mechanistic insight into how aging-related changes in the systemic environment drive impairments locally in the aged brain, and highlight the involvement of B2M and MHC I molecules in this process. From a translational perspective, our data raise the possibility that age-related cognitive and regenerative dysfunction observed during aging could be ameliorated by targeting B2M in old age.

Online methods

Animal Models

The following mouse lines were used: C57BL/6 (The Jackson Laboratory), C57BL/6 aged mice (National Institutes of Aging), *ß2-Microglobulin* (*B2m*$^{-/-}$) mutant mice and *transporter associated with antigen processing 1* (*Tap1*$^{-/-}$) mutant mice (The Jackson Laboratory). All studies were done in male mice. The numbers of mice used to result in statistically significant differences was calculated using standard power calculations with $\alpha = 0.05$ and a power of 0.8. We used an online tool (http://www.stat.uiowa.edu/~rlenth/Power/index.html) to calculate power and sample size based on experience with the respective tests, variability of the assays and inter-individual differences within groups. Mice were housed under specific pathogen-free conditions under a 12 h light-dark cycle and all animal handling and use was in accordance with institutional guidelines approved by the University of California San Francisco IACUC and the VA Palo Alto Committee on Animal Research.

Parabiosis

Parabiosis surgery followed previously described procedures[6,7]. Mirror-image incisions at the left and right flanks were made through the skin and shorter incisions were made through the abdominal wall. The peritoneal openings of the adjacent parabionts were sutured together. Elbow and knee joints from each parabiont were sutured together and the skin of each mouse was stapled (9mm Autoclip, Clay Adams) to the skin of the adjacent parabiont. Each mouse was injected subcutaneously with Baytril antibiotic and Buprenex as directed for pain and monitored during recovery. For overall health and maintenance behavior,

Author Manuscript Author Manuscript Author Manuscript Author Manuscript

several recovery characteristics were analyzed at various times after surgery, including paired weights and grooming behavior.

Stereotaxic injections

Animals were placed in a stereotaxic frame and anesthetized with 2% isoflurane (2L/min oxygen flow rate) delivered through an anesthesia nose cone. Ophthalmic eye ointment (Puralube Vet Ointment, Dechra) was applied to the cornea to prevent desiccation during surgery. The area around the incision was trimmed. Solutions were injected bilaterally into the DG of the dorsal hippocampi using the following coordinates: (from bregma) anterior = −2mm, lateral = 1.5mm, (from skull surface) height = −2.1mm. A 2 μl volume was injected stereotaxically over 10 minutes (injection speed: 0.20μl/min) using a 5 μl 26s gauge Hamilton syringe. To limit reflux along the injection track, the needle was maintained *in situ* for 8 minutes, slowly pulled out half way and kept in position for an additional two minutes. The skin was closed using silk suture. Each mouse was injected subcutaneously with the analgesic Buprenex. Mice were single-housed and monitored during recovery.

B2M administration

Carrier free purified human β2-Microglobulin (Lee Biosolutions) was dissolved in PBS and administered systemically (100 ug/kg) via intraorbital injections in young (3 months) wild type animals, or stereotaxically (0.50ul; 0.1ug/ul) into the DG of the hippocampus in young (3 months) wild type and *Tap1*$^{-/-}$ mice. For histological analysis B2M and vehicle were administered into contralateral DG of the same animal. For behavioral analysis B2M or vehicle were administered bilaterally into the DG and mice were allowed to recover for six or 30 days prior to cognitive testing.

BrdU administration and quantification

For short term Brdu labeling 50 mg/kg of BrdU was injected intraperitoneally into mice daily either three or six days before sacrifice. For long term BrdU labeling 50 mg/kg of BrdU was injected into mice once a day for six days and animals were sacrificed 28 days after first administration. To estimate the total number of BrdU-positive cells in the brain, we performed DAB staining for BrdU on every sixth hemibrain section for a total of six sections. The number of BrdU-positive cells in the granule cell and subgranular cell layer of the DG were counted and multiplied by 12 to estimate the total number of BrdU-positive cells in the entire DG. To determine the fate of dividing cells a total of 200 BrdU-positive cells across 4–6 sections per mouse were analyzed by confocal microscopy for co-expression with NeuN and GFAP. The number of double-positive cells was expressed as a percentage of BrdU-positive cells.

Immunohistochemistry

Tissue processing and immunohistochemistry was performed on free-floating sections following standard published techniques[6]. Briefly, mice were anesthetized with 400 mg/kg chloral hydrate (Sigma-Aldrich) and transcardially perfused with 0.9% saline. Brains were removed and fixed in phosphate-buffered 4% paraformaldehyde, pH 7.4, at 4°C for 48 h before they were sunk through 30% sucrose for cryoprotection. Brains were then sectioned

Author Manuscript Author Manuscript Author Manuscript Author Manuscript

coronally at 40 μm with a cryomicrotome (Leica Camera, Inc.) and stored in cryoprotective medium. Primary antibodies were: goat anti-Dcx (1:500; Santa Cruz Biotechnology; sc-8066, clone: C-18), rat anti-BrdU (1:5000, Accurate Chemical and Scientific Corp.; ab6326, clone: BU1/75), mouse anti-Nestin (1:500; Millipore; MAB353; clone: rat-401), MCM2 (1:500, BD Biosciences; 610700; clone: 46/BM28), chicken anti-Tbr2 (1:500; Millipore; AB15894), mouse anti-NeuN (1:1000; Millipore; MAB377; clone: A60), rabbit anti-GFAP (1:500; DAKO; Z0334). After overnight incubation, primary antibody staining was revealed using biotinylated secondary antibodies (Vector) and the ABC kit (Vector) with Diaminobenzidine (DAB, Sigma-Aldrich) or fluorescence conjugated secondary antibodies (Life Technologies). For BrdU labeling, brain sections were pre-treated with 2N HCl at 37°C for 30 min and washed three times with Tris-Buffered Saline with Tween (TBST) before incubation with primary antibody. For Nestin and Tbr2 labeling, brain sections were pre-treated three times with 0.1M Citrate at 95°C for 5 min and washed three times with Tris-Buffered Saline with Tween (TBST) before incubation with primary antibody. To estimate the total number of Dcx positive cells per DG immunopositive cells in the granule cell and subgranular cell layer of the DG were counted in every sixth coronal hemibrain section through the hippocampus for a total of six sections and multiplied by 12.

Western Blot Analysis

Mouse hippocampi were dissected after perfusion of animals, snap frozen and lysed in RIPA lysis buffer (500 mM Tris, pH 7.4, 150 mM NaCl, 0.5% Na deoxycholate, 1% NP40, 0.1% SDS, and complete protease inhibitors; Roche). Tissue lysates were mixed with 4× NuPage LDS loading buffer (Invitrogen) and loaded on a 4–12% SDS polyacrylamide gradient gel (Invitrogen) and subsequently transferred onto a nitrocellulose membrane. The blots were blocked in 5% milk in Tris-Buffered Saline with Tween (TBST) and incubated with rabbit anti-actin (1:5000, Sigma; A5060) and rabbit anti-B2M (1:2500, Abcam; ab75853; clone: EP2978Y). Horseradish peroxidase-conjugated secondary antibodies (1:5000, GE Healthcare; NA934) and an ECL kit (GE Healthcare/Amersham Pharmacia Biotech) were used to detect protein signals. Multiple exposures were taken to select images within the dynamic range of the film (GE Healthcare Amersham HyperfilmTM ECL). Selected films were scanned (300 dpi) and quantified using ImageJ software (Version 1.46k). Actin bands were used for normalization.

Cell culture assays

Mouse neural progenitor cells were isolated from C57BL/6 mice or Dcx-reporter mice[37] as previously described[6,38]. Brains from postnatal animals (1 day-old) were dissected to remove olfactory bulbs, cortex, cerebellum and brainstem. After removing superficial blood vessels hippocampi were finely minced with a scalpel, digested for 30 minutes at 37°C in DMEM media containing 2.5U/ml Papain (Worthington Biochemicals), 1U/ml Dispase II (Boeringher Mannheim), and 250U/ml DNase I (Worthington Biochemicals) and mechanically dissociated. NSC/progenitors were purified using a 65% Percoll gradient and plated on uncoated tissue culture dishes at a density of 10^5 cells/cm^2. NPCs were cultured under standard conditions for 48 hours in NeuroBasal A medium supplemented with penicillin (100U/ml), streptomycin (100mg/ml), 2 mM L-glutamine, serum-free B27 supplement without vitamin A (Sigma-Aldrich), bFGF (20ng/ml) and EGF (20ng/ml).

Author Manuscript Author Manuscript Author Manuscript Author Manuscript

Carrier free forms of human recombinant B2M (Vendor) were dissolved in PBS and added to cell cultures under self-renewal conditions every other day following cell plating. For proliferation BrdU incorporation was measured using a cell proliferation assay system that uses a peroxidase-coupled anti-BrdU antibody together with a color substrate for detection (Fisher). For bioluminescence assays Dcx-luciferase activity was measured using a luciferase assay system (Promega). Differentiation was assessed by immunocytochemistry using mouse anti-MAP2 (1:1000, Sigma; M9942; clone: HM-2) and rabbit anti-GFAP (1:500, DAKO; Z0334) antibodies. Cytotoxicity was measured by lactate dehydrogenase (LDH) detection using a Pierce LDH Cytotoxicity Assay system (Life Technologies).

Contextual Fear Conditioning

In this task, mice learned to associate the environmental context (fear conditioning chamber) with an aversive stimulus (mild foot shock; unconditioned stimulus, US) enabling testing for hippocampal-dependent contextual fear conditioning. As contextual fear conditioning is hippocampus and amygdala dependent, the mild foot shock was paired with a light and tone cue (conditioned stimulus, CS) in order to also assess amygdala-dependent cued fear conditioning. Conditioned fear was displayed as freezing behavior. Specific training parameters are as follows: tone duration is 30 seconds; level is 70 dB, 2 kHz; shock duration is 2 seconds; intensity is 0.6 mA. This intensity is not painful and can easily be tolerated but will generate an unpleasant feeling. More specifically, on day 1 each mouse was placed in a fear-conditioning chamber and allowed to explore for 2 minutes before delivery of a 30-second tone (70 dB) ending with a 2-second foot shock (0.6mA). Two minutes later, a second CS-US pair was delivered. On day 2 each mouse was first place in the fear-conditioning chamber containing the same exact context, but with no CS or foot shock. Freezing was analyzed for 1–3 minutes. One hour later, the mice were placed in a new context containing a different odor, cleaning solution, floor texture, chamber walls and shape. Animals were allowed to explore for 2 minutes before being re-exposed to the CS. Freezing was analyzed for 1–3 minutes. Freezing was measured using a FreezeScan video tracking system and software (Cleversys, Inc).

Radial Arm Water Maze

Spatial learning and memory was assessed using the radial arm water maze (RAWM) paradigm following the protocol described by Alamed et al.[39]. In this task the goal arm location containing a platform remains constant throughout the training and testing phase, while the start arm is changed during each trial. On day one during the training phase, mice are trained for 15 trails, with trials alternating between a visible and hidden platform. On day two during the testing phase, mice are tested for 15 trials with a hidden platform. Entry into an incorrect arm is scored as an error, and errors are averaged over training blocks (three consecutive trials). Investigators were blinded to genotype and treatment when scoring.

Plasma collection and proteomic analysis

Mouse blood was collected into EDTA coated tubes via tail vein bleed, mandibular vein bleed, or intracardial bleed at time of sacrifice. EDTA plasma was generated by centrifugation at 1000g of freshly collected blood and aliquots were stored at −80°C until use. Human plasma and CSF samples were obtained from University of Washington School

Author Manuscript Author Manuscript Author Manuscript Author Manuscript

of Medicine, Veterans Affairs Northwest Network Mental Illness Research, Education, and Clinical Center, Oregon Health Science University and University of California San Diego. Subjects were chosen based on standardized inclusion and exclusion criteria as previously described[6,40,41] and outlined in Supplementary Table 1. Informed consent was obtained from human subjects according to the institutional review board guidelines at the respective centers. The plasma concentrations of cytokines and signaling molecules were measured in human and mouse plasma samples using standard antibody-based multiplex immunoassays (Luminex) by Rules Based Medicine Inc., a fee-for-service provider. All Luminex measurements where obtained in a blinded fashion. All assays were developed and validated to Clinical Laboratory Standards Institute (formerly NCCLS) guidelines based upon the principles of immunoassay as described by the manufacturers.

Data and statistical analyses

All experiments were randomized and blinded by an independent researcher prior to pharmacological treatment or assessment of genetic mouse models. Researchers remained blinded throughout histological, biochemical and behavioral assessments. Groups were un-blinded at the end of each experiment upon statistical analysis. Data are expressed as mean ± SEM. The distribution of data in each set of experiments was tested for normality using D'Agostino-Pearson omnibus test or Shapiro-Wilk test. No significant differences in variance between groups were detected using an F test. Statistical analysis was performed with Prism 5.0 software (GraphPad Software). Means between two groups were compared with two-tailed, unpaired Student's t test. Comparisons of means from multiple groups with each other or against one control group were analyzed with 1-way ANOVA followed by appropriate post-hoc tests (indicated in figure legends).

Supplementary Material

Refer to Web version on PubMed Central for supplementary material.

Acknowledgments

We thank D.R. Galasko (University of California San Diego), J.A. Kaye (Oregon Health Sciences University), G. Li (Veterans Affairs Northwest Network Mental Illness Research, Education, and Clinical Center), E.R. Peskind (University of Washington and Veterans Affairs Northwest Network Mental Illness Research, Education, and Clinical Center), and J.F. Quinn (Oregon Health Sciences University) for generously providing human plasma and CSF samples. We are grateful to numerous unnamed human subjects and staff for their contributions. We thank D. Dubal and M. Thomson for critically reading manuscript. This work was funded by CIRM fellowship (K.L.), NSF fellowship (J.U), NRSA fellowship (1F31-AG050415, E.G.W), Anonymous (T.W.-C), Veterans Affairs (T.W.-C), NIA (AG027505, T.W.-C), CIRM (T.W.-C), Sandler Foundation (S.A.V), gift from Marc and Lynne Benioff, (S.A.V.), UCSF-CTSI (UL1-TR000004, S.A.V), NIH Director's Independence Award (DP5-OD12178, S.A.V).

References

1. Hedden T, Gabrieli JD. Insights into the ageing mind: a view from cognitive neuroscience. Nature reviews. Neuroscience. 2004; 5:87–96. [PubMed: 14735112]
2. Mattson MP, Magnus T. Ageing and neuronal vulnerability. Nature reviews. Neuroscience. 2006; 7:278–294. [PubMed: 16552414]
3. Small SA, Schobel SA, Buxton RB, Witter MP, Barnes CA. A pathophysiological framework of hippocampal dysfunction in ageing and disease. Nature reviews. Neuroscience. 2011; 12:585–601. [PubMed: 21897434]

Author Manuscript Author Manuscript Author Manuscript Author Manuscript

4. Rao MS, Hattiangady B, Shetty AK. The window and mechanisms of major age-related decline in the production of new neurons within the dentate gyrus of the hippocampus. Aging cell. 2006; 5:545–558. [PubMed: 17129216]
5. Katsimpardi L, et al. Vascular and neurogenic rejuvenation of the aging mouse brain by young systemic factors. Science. 2014; 344:630–634. [PubMed: 24797482]
6. Villeda SA, et al. The ageing systemic milieu negatively regulates neurogenesis and cognitive function. Nature. 2011; 477:90–94. [PubMed: 21886162]
7. Villeda SA, et al. Young blood reverses age-related impairments in cognitive function and synaptic plasticity in mice. Nature medicine. 2014; 20:659–663.
8. Ruckh JM, et al. Rejuvenation of regeneration in the aging central nervous system. Cell stem cell. 2012; 10:96–103. [PubMed: 22226359]
9. Conboy IM, et al. Rejuvenation of aged progenitor cells by exposure to a young systemic environment. Nature. 2005; 433:760–764. [PubMed: 15716955]
10. Brack AS, et al. Increased Wnt signaling during aging alters muscle stem cell fate and increases fibrosis. Science. 2007; 317:807–810. [PubMed: 17690295]
11. Laviano A. Young blood. The New England journal of medicine. 2014; 371:573–575. [PubMed: 25099584]
12. Bouchard J, Villeda SA. Aging and brain rejuvenation as systemic events. Journal of neurochemistry. 2014
13. Zijlstra M, et al. Beta 2-microglobulin deficient mice lack CD4-8+ cytolytic T cells. Nature. 1990; 344:742–746. [PubMed: 2139497]
14. Lee H, et al. Synapse elimination and learning rules co-regulated by MHC class I H2-Db. Nature. 2014; 509:195–200. [PubMed: 24695230]
15. Loconto J, et al. Functional expression of murine V2R pheromone receptors involves selective association with the M10 and M1 families of MHC class Ib molecules. Cell. 2003; 112:607–618. [PubMed: 12628182]
16. Boulanger LM, Shatz CJ. Immune signalling in neural development, synaptic plasticity and disease. Nature reviews. Neuroscience. 2004; 5:521–531. [PubMed: 15208694]
17. Shatz CJ. MHC class I: an unexpected role in neuronal plasticity. Neuron. 2009; 64:40–45. [PubMed: 19840547]
18. Huh GS, et al. Functional requirement for class I MHC in CNS development and plasticity. Science. 2000; 290:2155–2159. [PubMed: 11118151]
19. Goddard CA, Butts DA, Shatz CJ. Regulation of CNS synapses by neuronal MHC class I. Proceedings of the National Academy of Sciences of the United States of America. 2007; 104:6828–6833. [PubMed: 17420446]
20. Glynn MW, et al. MHCI negatively regulates synapse density during the establishment of cortical connections. Nature neuroscience. 2011; 14:442–451. [PubMed: 21358642]
21. Murray AM. Cognitive impairment in the aging dialysis and chronic kidney disease populations: an occult burden. Advances in chronic kidney disease. 2008; 15:123–132. [PubMed: 18334236]
22. Corlin DB, et al. Quantification of cleaved beta2-microglobulin in serum from patients undergoing chronic hemodialysis. Clinical chemistry. 2005; 51:1177–1184. [PubMed: 15890888]
23. McArthur JC, et al. The diagnostic utility of elevation in cerebrospinal fluid beta 2-microglobulin in HIV-1 dementia. Multicenter AIDS Cohort Study. Neurology. 1992; 42:1707–1712. [PubMed: 1355286]
24. Brew BJ, Dunbar N, Pemberton L, Kaldor J. Predictive markers of AIDS dementia complex: CD4 cell count and cerebrospinal fluid concentrations of beta 2-microglobulin and neopterin. The Journal of infectious diseases. 1996; 174:294–298. [PubMed: 8699058]
25. Carrette O, et al. A panel of cerebrospinal fluid potential biomarkers for the diagnosis of Alzheimer's disease. Proteomics. 2003; 3:1486–1494. [PubMed: 12923774]
26. Clelland CD, et al. A functional role for adult hippocampal neurogenesis in spatial pattern separation. Science. 2009; 325:210–213. [PubMed: 19590004]
27. Kitamura T, et al. Adult neurogenesis modulates the hippocampus-dependent period of associative fear memory. Cell. 2009; 139:814–827. [PubMed: 19914173]

Author Manuscript Author Manuscript Author Manuscript Author Manuscript

28. Zhang CL, Zou Y, He W, Gage FH, Evans RM. A role for adult TLX-positive neural stem cells in learning and behaviour. Nature. 2008; 451:1004–1007. [PubMed: 18235445]
29. Drapeau E, et al. Spatial memory performances of aged rats in the water maze predict levels of hippocampal neurogenesis. Proceedings of the National Academy of Sciences of the United States of America. 2003; 100:14385–14390. [PubMed: 14614143]
30. Merrill DA, Karim R, Darraq M, Chiba AA, Tuszynski MH. Hippocampal cell genesis does not correlate with spatial learning ability in aged rats. The Journal of comparative neurology. 2003; 459:201–207. [PubMed: 12640670]
31. Bizon JL, Gallagher M. Production of new cells in the rat dentate gyrus over the lifespan: relation to cognitive decline. The European journal of neuroscience. 2003; 18:215–219. [PubMed: 12859354]
32. Seib DR, et al. Loss of Dickkopf-1 restores neurogenesis in old age and counteracts cognitive decline. Cell stem cell. 2013; 12:204–214. [PubMed: 23395445]
33. Van Kaer L, Ashton-Rickardt PG, Ploegh HL, Tonegawa S. TAP1 mutant mice are deficient in antigen presentation, surface class I molecules, and CD4-8+ T cells. Cell. 1992; 71:1205–1214. [PubMed: 1473153]
34. Laguna Goya R, Tyers P, Barker RA. Adult neurogenesis is unaffected by a functional knock-out of MHC class I in mice. Neuroreport. 2010; 21:349–353. [PubMed: 20147861]
35. Adelson JD, et al. Neuroprotection from stroke in the absence of MHCI or PirB. Neuron. 2012; 73:1100–1107. [PubMed: 22445338]
36. Jeck WR, Siebold AP, Sharpless NE. Review: a meta-analysis of GWAS and age-associated diseases. Aging cell. 2012; 11:727–731. [PubMed: 22888763]
37. Couillard-Despres S, et al. In vivo optical imaging of neurogenesis: watching new neurons in the intact brain. Molecular imaging. 2008; 7:28–34. [PubMed: 18384721]
38. Mosher KI, et al. Neural progenitor cells regulate microglia functions and activity. Nature neuroscience. 2012; 15:1485–1487. [PubMed: 23086334]
39. Alamed J, Wilcock DM, Diamond DM, Gordon MN, Morgan D. Two-day radial-arm water maze learning and memory task; robust resolution of amyloid-related memory deficits in transgenic mice. Nature protocols. 2006; 1:1671–1679. [PubMed: 17487150]
40. Zhang J, et al. CSF multianalyte profile distinguishes Alzheimer and Parkinson diseases. American journal of clinical pathology. 2008; 129:526–529. [PubMed: 18343778]
41. Li G, et al. Cerebrospinal fluid concentration of brain-derived neurotrophic factor and cognitive function in non-demented subjects. PloS one. 2009; 4:e5424. [PubMed: 19412541]

Author Manuscript Author Manuscript Author Manuscript Author Manuscript

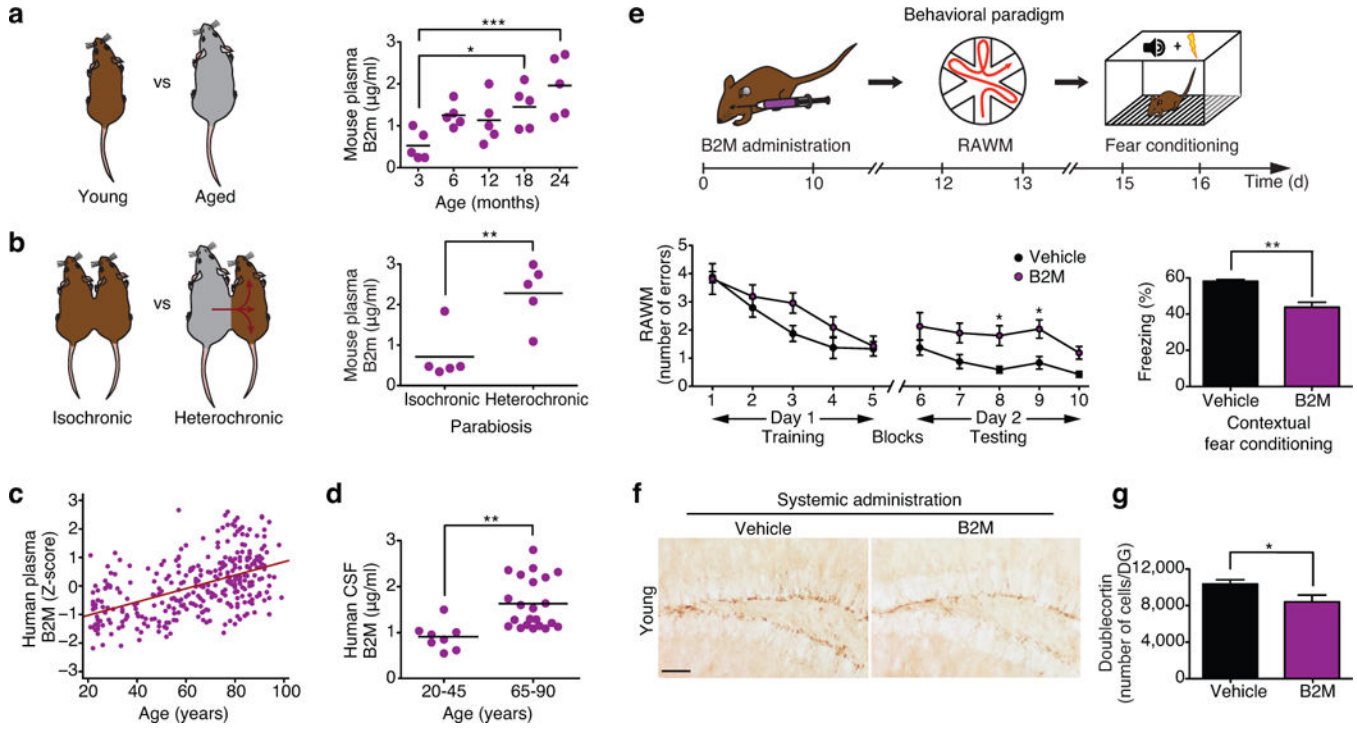

Figure 1. Systemic B2M increases with age and impairs hippocampal-dependent cognitive function and neurogenesis

a,b, Schematic of unpaired young versus aged mice (**a**), and young isochronic versus heterochronic parabionts (**b**). Changes in plasma concentration of B2m with age at 3, 6, 12, 18 and 24 months (**a**) and between young isochronic and young heterochronic parabionts five weeks after parabiosis (**b**). Data from 5 mice per group. **c,d,** Changes in plasma (**c;** r=0.51; p<0.0001; 95% confidence interval=0.19–0.028) and CSF (**d**) B2M concentrations with age in healthy human subjects. Data from 318 individuals (**c**), 8 young (20–45) individuals (**d**), and 22 old (65–90) individuals (**d**). **e,** Young adult (3 months) mice were injected intraorbitally with B2M or PBS (vehicle) control five times over 12 days. **e,** Schematic of chronological order used for B2M treatment and cognitive testing. **e,** Hippocampal learning and memory assessed by RAWM (number of entry arm errors prior to finding platform) and contextual fear conditioning (percent freezing time 24h after training). Data from 10 mice per group. **f,** Representative field of Dcx-positive cells for each treatment group (scale bar: 100μm). **g,** Quantification of neurogenesis in the dentate gyrus (DG) after treatment. Data from 7 B2M treated and 8 vehicle treated mice. All data represented as dot plots with Mean or bar graphs with Mean±SEM; **P* < 0.05; ***P* < 0.01; ****P* < 0.001 t-test (**b,d,e,g**), ANOVA, Tukey's post-hoc test (**a**), Mann-Whitney U Test (**c**) and repeated measures ANOVA, Bonferroni post-hoc test (**e**).

Author Manuscript Author Manuscript Author Manuscript Author Manuscript

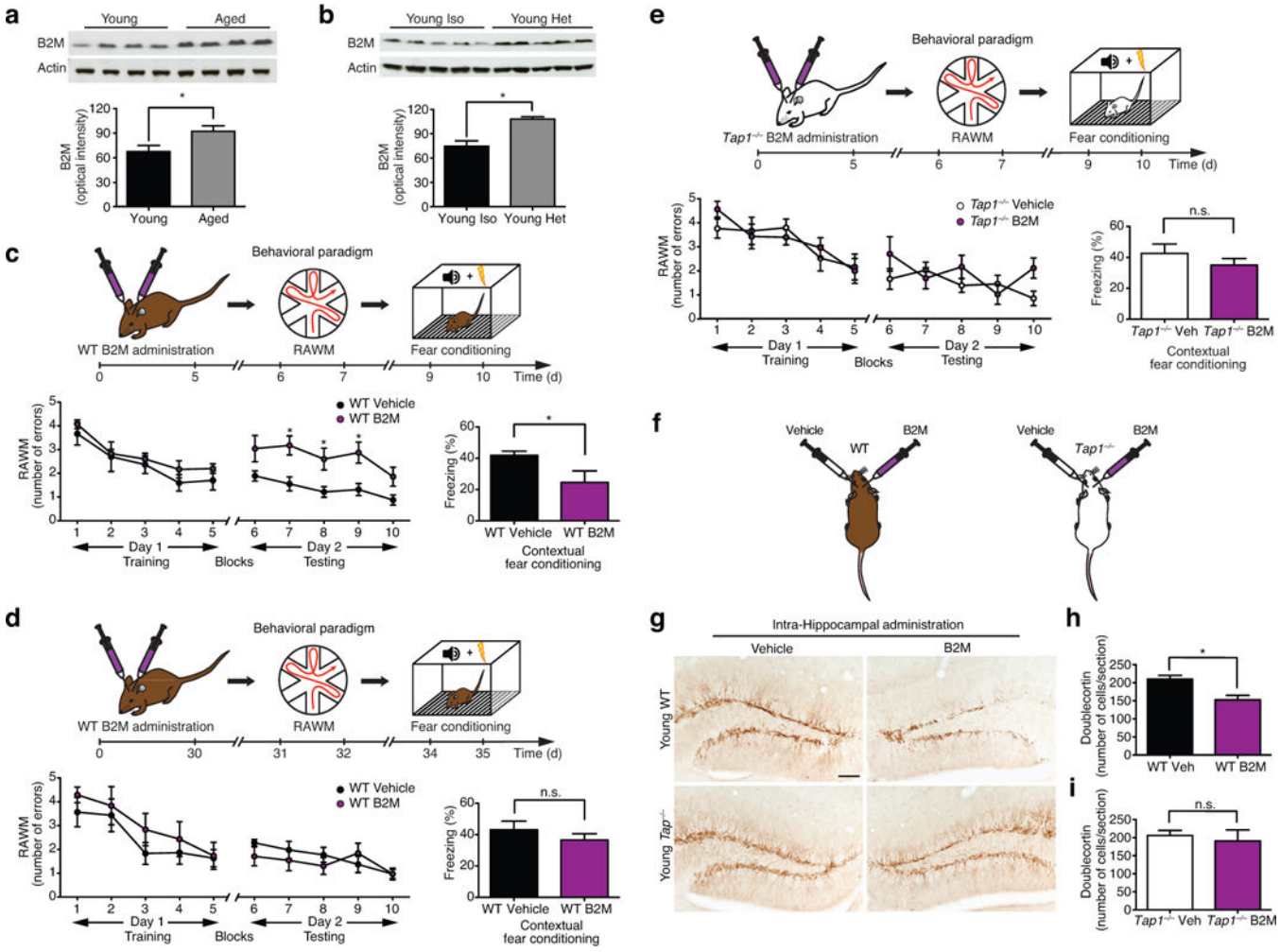

Figure 2. B2M expression increases in the aging hippocampus and impairs hippocampal-dependent cognitive function and neurogenesis

a,b, Representative Western blot and quantification of hippocampal lysates probed with anti-B2m and anti-Actin antibodies from young (3 months) and aged (18 months) unpaired animals (**a**), or young isochronic and young heterochronic parabionts five weeks after parabiosis (**b**). **c–e**, Young (3 months) adult wild type (WT; **c,d**) or Tap1-deficient (**e**) mice were given bilateral stereotaxic injections of B2M or vehicle six days (**c,e**) or 30 days (**d**) prior to behavioral testing. **c–e**, Schematics illustrating chronological order used for local B2M administration and cognitive testing. **c–e**, Learning and memory as assessed by RAWM and contextual fear conditioning following stereotaxic injections. Data from 10 animals per genotype and treatment group. **f–i,** Young adult (3 months) WT and *Tap1*$^{-/-}$ mice were given unilateral stereotaxic injections of B2M or vehicle control. **f**, Schematic illustrating injection paradigm. **g,** Representative field of Dcx-positive cells in adjacent sides of the DG within the same section are shown for WT and *Tap1*$^{-/-}$ treatment groups. **h,i,** Quantification of neurogenesis in the DG of WT (**h**) and *Tap1*$^{-/-}$ (**i**) mice after stereotaxic B2M administration. Data from five mice per genotype and treatment group. All data represented as Mean±SEM; **P*<0.05; ***P*<0.01; n.s. not significant; ANOVA, t-test (**a–e,h,i**); repeated measures ANOVA, Bonferroni post-hoc test (**c–e**).

Author Manuscript Author Manuscript Author Manuscript Author Manuscript

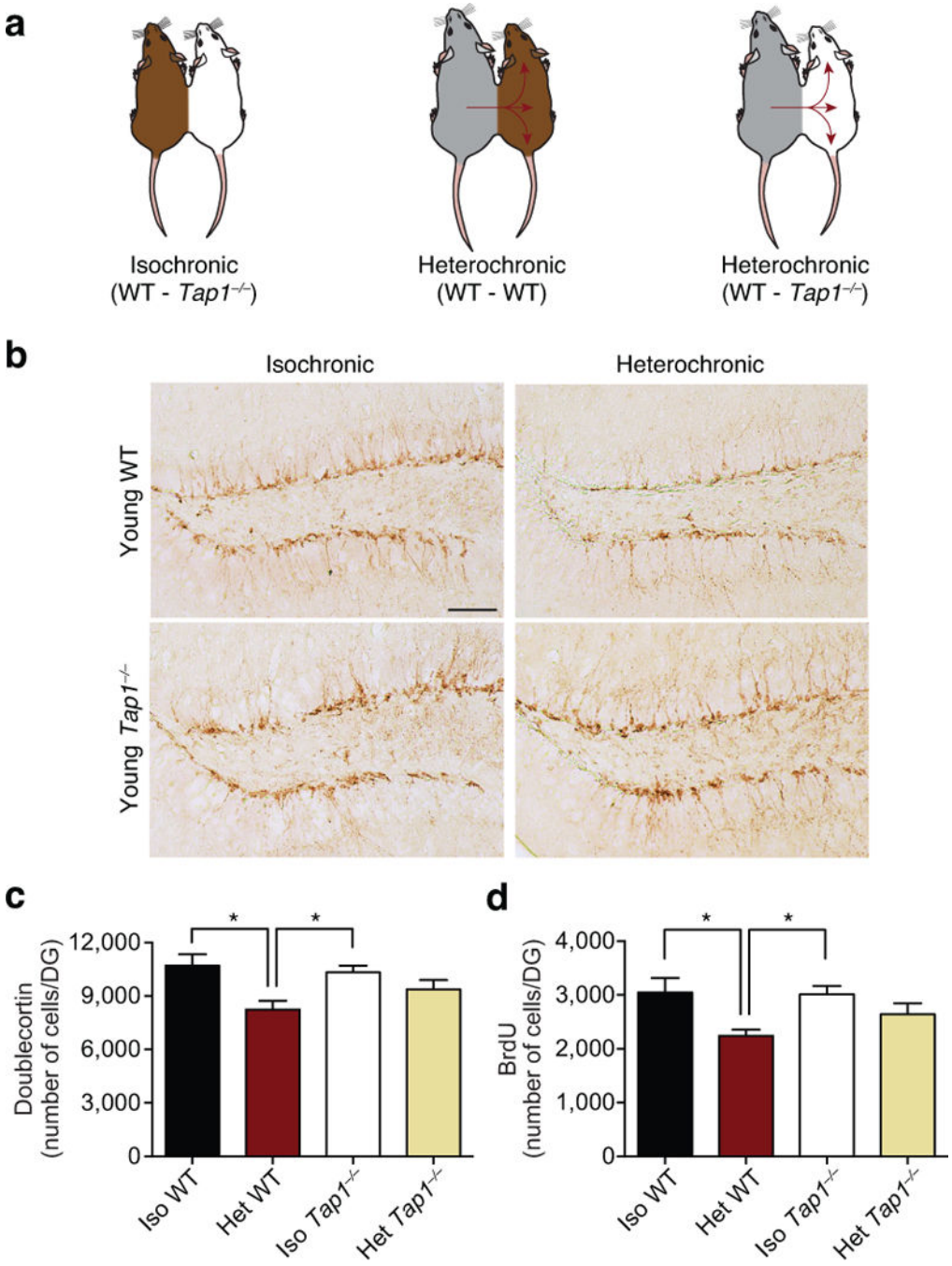

Figure 3. Reducing MHC I surface expression mitigates the negative effects of heterochronic parabiosis on neurogenesis

a, Schematic of young (3 months) wild type (WT) and *Tap1*$^{-/-}$ isochronic parabionts and young WT and *Tap1*$^{-/-}$ heterochronic parabionts. **b,c** Representative images of the dentate gyrus (**b**) and quantification (**c**) of Doublecortin immunostaining of young isochronic and heterochronic parabionts five weeks after parabiosis (arrowheads point to individual cells, scale bar: 100μm). **d,** Prior to euthanasia animals were injected with Bromodeoxyuridine (BrdU) for three days, and proliferating cells having incorporated BrdU were quantified in

DG after parabiosis. Data from 8 young isochronic WT, 6 young isochronic *Tap1*$^{-/-}$, 8 young heterochronic WT, and 8 young heterochronic *Tap1*$^{-/-}$ parabionts. All data represented as Mean±SEM; **P*< 0.05; ANOVA, Tukey's post-hoc test.

Author Manuscript Author Manuscript Author Manuscript Author Manuscript

Author Manuscript Author Manuscript Author Manuscript Author Manuscript

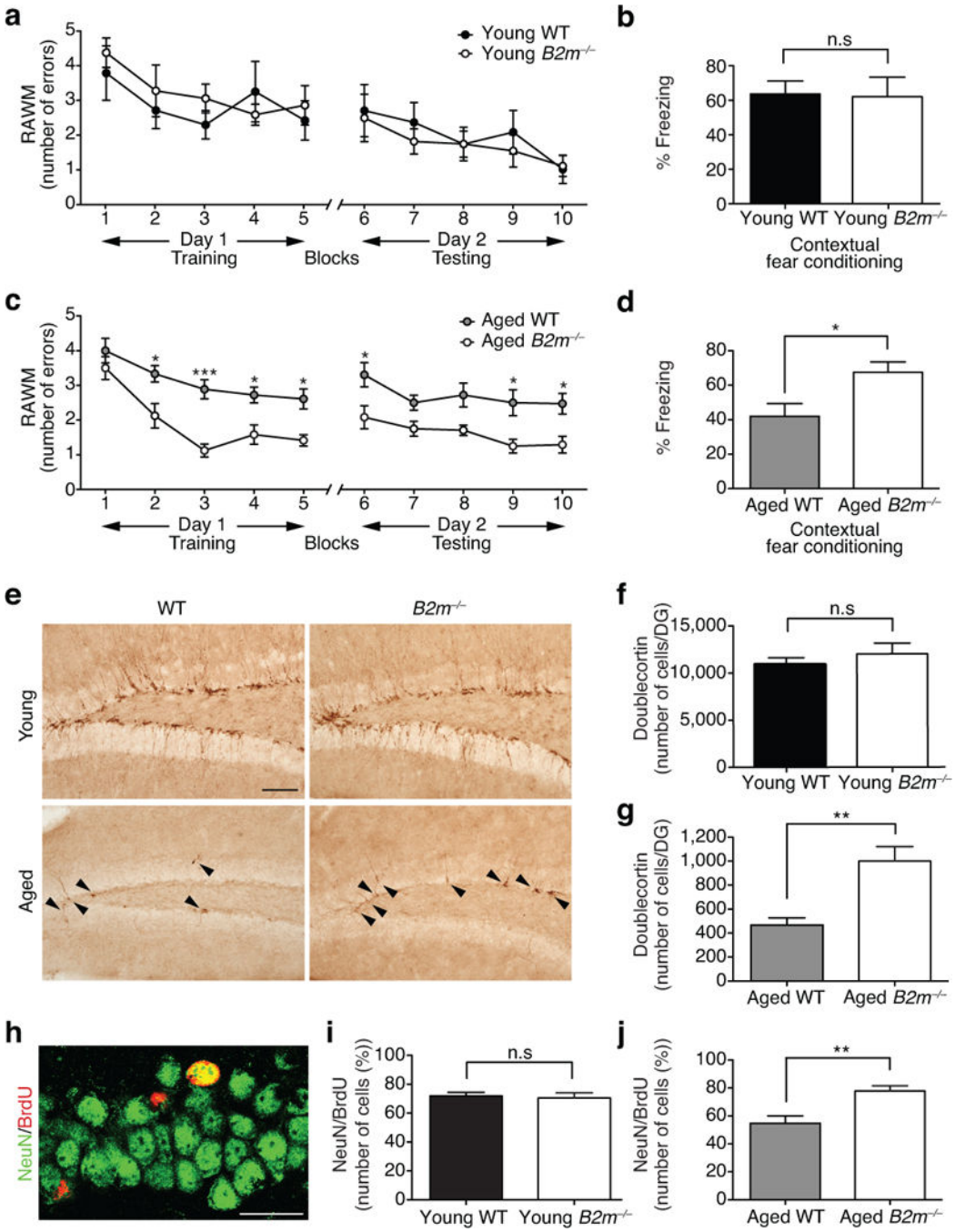

Figure 4. Absence of B2m enhances hippocampal-dependent cognitive function and neurogenesis in aged animals

a–d, Learning and memory in young (3 months) and aged (17 months) wild type (WT) and B2m knockout ($B2m^{-/-}$) mice by RAWM (**a,c**) and contextual fear conditioning (**b,d**). Data from 10 young WT, 10 young $B2m^{-/-}$, 8 aged WT, and 12 aged $B2m^{-/-}$ mice. **e–j,** Neurogenesis as assessed by immunostaining for Dcx-positive cells in the DG of young and aged WT and $B2m^{-/-}$ mice. Representative field and quantification of Dcx-positive cells are shown for young (**e,f**) and aged (**e,g**) WT and $B2m^{-/-}$ animals (arrowheads point to

Author Manuscript Author Manuscript Author Manuscript Author Manuscript

individual immature neurons, scale bar: 100μm). Data from 8 young and 10 aged mice per genotype. **h–j**, WT and *B2m*$^{-/-}$ mice were administered BrdU by intraperitoneal injections for six days and euthanized 28 days later. **h**, Representative confocal images from the DG of brain sections immunostained for BrdU (red) in combination with NeuN (green; scale bar: 25μm). **i,j**, Quantification of the relative number of BrdU and NeuN-double positive cells out of the total BrdU-positive cells in the young (**i**) and aged (**j**) DG of WT and *B2m*$^{-/-}$ animals. Data from 8 mice per group (3 sections per mouse). All data represented as Mean ±SEM; **P*< 0.05; ***P*<0.01; n.s. not significant; t-test (**b,d,f,i,j**); repeated measures ANOVA, Bonferroni post-hoc test (**a,c**).